



REVIEW ARTICLE

MC1R and melanin-based molecular probes for theranostic of melanoma and beyond

Hui Shi¹ and Zhen Cheng^{1,2,3}

Malignant melanoma is accounting for most of skin cancer-associated mortality. The incidence of melanoma increased every year worldwide especially in western countries. Treatment efficiency is highly related to the stage of melanoma. Therefore, accurate staging and restaging play a pivotal role in the management of melanoma patients. Though ¹⁸F-fluorodeoxyglucose (¹⁸F-FDG) positron-emission tomography (PET) has been widely used in imaging of tumor metastases, novel radioactive probes for specific targeted imaging of both primary and metastasized melanoma are still desired. Melanocortin receptor 1 (MC1R) and melanin are two promising biomarkers specifically for melanoma, and numerous research groups including us have been actively developing a plethora of radioactive probes based on targeting of MC1R or melanin for over two decades. In this review, some of the MC1R-targeted tracers and melanin-associated molecular imaging probes developed in our research and others have been briefly summarized, and it provides a quick glance of melanoma-targeted probe design and may contribute to further developing novel molecular probes for cancer theranostics.

Keywords: melanoma; molecular probes; radiotracers; MC1R; melanin

Acta Pharmacologica Sinica (2022) 43:3034–3044; <https://doi.org/10.1038/s41401-022-00970-y>

INTRODUCTION

Malignant melanoma is the most lethal form of skin cancer, accounting for ~73% of skin cancer-related deaths, although its annual diagnosis is less than 5% of all skin cancers [1, 2]. Moreover, the incidence of melanoma continues to increase worldwide [3–8], and the incidence rate at 2021 was 6 times as high as that of 40 years ago [9]. Most melanoma patients with local disease (stage I & II) are curable by resection surgery and the 5-year relative survival rate reaches 99% in recent years [10]. Unfortunately, it drops significantly for advanced or metastatic melanoma (stage IV) patients (68% for regional and 30% for distant melanoma lesions), because of limitation of the current treatment options and staging strategies [11–13].

Compared to other tumors, primary melanoma with cutaneous location permits its advantages in detection. The ABCD (representing Asymmetry, Border irregularity, Color variegation, and Diameter >6 mm, respectively) acronym for the appraisal of cutaneous pigmented lesions is widely used to facilitate the early diagnosis of melanoma [14, 15]. Generally, susceptible cutaneous melanoma patients need to be further diagnosed with microscopy and confirmed by histological examination [4, 16]. The prognosis of melanoma is directly proportionate to the depth of the neoplasm [15, 17–20]. While these conventional procedures are confronted with the limitations for identifying systemic melanoma, especially in asymptomatic patients with metastasis [21, 22]. Therefore, non-invasive whole-body imaging strategies with the capacity of early and accurate diagnosis, such as single-photon emission computed tomography (SPECT) and positron-emission tomography (PET), are

key for staging patients and formulating appropriate treatment strategies to realize the best possible prognosis [21, 23].

In clinical practice today, ¹⁸F-fluorodeoxyglucose (¹⁸F-FDG) is used in the assessment of both metabolic and anatomic characteristics of the primary melanoma tumor and its potential small nodal and visceral metastases [24, 25]. But ¹⁸F-FDG-PET may have limited utilities for the detection of nodal micro-metastases (<5 mm) and non-metabolically active lesions [26, 27]. Moreover, the tumor-targeting ability of ¹⁸F-FDG is involved in the glucose metabolism, which is also increased in multiple diseases, thus ¹⁸F-FDG is not a specific targeted PET probe for malignant tumors [22, 28, 29]. Therefore, developing molecularly targeted probes is still desired, and such probes can play a pivotal role in diagnosing and accurate staging of metastatic melanoma.

Melanocortin receptor 1 (MC1R) and melanin are two promising targets that overexpressed in the most of melanoma cells, and they serve as attractive targets for developing specific molecular probes [30]. In this mini review, we mainly summarized some work and the progress of the development of MC1R and melanin-associated radiotracers.

MC1R-ASSOCIATED RADIOTRACERS

MC1R also known as α -melanocyte-stimulating hormone (α -MSH) receptor is a seven-pass transmembrane G-protein coupled receptor of 317 amino acids, and it is a key regulator of pigmentation expressed in skin melanocytes [31]. Some of MC1R variants can increase the risk for malignant melanoma, and

¹State Key Laboratory of Drug Research, Molecular Imaging Center, Shanghai Institute of Materia Medica, Chinese Academy of Sciences, Shanghai 201203, China; ²University of Chinese Academy of Sciences, No. 19A Yuquan Road, Beijing 100049, China and ³Shandong Laboratory of Yantai Drug Discovery, Bohai Rim Advanced Research Institute for Drug Discovery, Yantai 264117, China

Correspondence: Zhen Cheng (zcheng@simm.ac.cn)

Received: 19 June 2022 Accepted: 27 July 2022

Published online: 25 August 2022

multiple molecular and pathological processes can be promoted after MC1R binding with α -MSH, such as activating 3',5'-cyclic adenosine monophosphate (cAMP) signaling, enhancing melanin production in melanocytes, and stimulating DNA-damage repair [32–38]. Previous studies have indicated that MC1R was over-expressed in vast majority of human melanomas both primary and metastatic lesions [16, 39, 40]. As MC1R is an important biomarker in melanoma, its natural binding ligand α -MSH and analogs have been studied as attractive molecular platforms for developing melanoma-targeted probes.

α -MSH (Ac-SYSMEHFRWGKPV-NH₂) is a tridecapeptide cleaved by prohormone convertase 2 from POMC (proopiomelanocortin) precursor [41, 42], and it exhibits high binding affinity with MC1R ($K_D = 1.35 \pm 0.5$ nM) [43]. But like many other endogenous peptides, it is unstable in human with the half-life less than 3 min [44, 45]. Therefore, various α -MSH analogs have been developed based on its minimum active sequence for MC1R (His⁶-Phe⁷-Arg⁸-Trp⁹) with the aim for enhancement of peptide stability, specificity, and affinity [46, 47]. Among them, most of α -MSH analogs can be categorized into two groups, linear α -MSH analogs, and cyclized α -MSH analogs. Tremendous work has been undertaken over the past decades for developing radiotracers based on α -MSH analogs (Table 1) [45, 48–50].

Modifying α -MSH derivatives with unnatural amino acid substitutions is a conventional strategy to improve their stability. The classic linear α -MSH analogs can be represented by NDP ([Nle⁴, d-Phe⁷]- α -MSH) and NAPamide ([Nle⁴, Asp⁵, d-Phe⁷, Lys¹¹]- α -MSH^{4–11}), which both have prolonged activity. After labeled by radionuclides, these linear α -MSH analogs show high affinity to MC1R and relatively good biodistribution performance [51–55]. Cyclization is another widely used approach for α -MSH peptide modification making them better fit the MC1R-binding pocket for improved binding affinities as well as in vivo stability, that can be realized with disulfide bonds, thiolate–metal–thiolate bridges, lactam linkages, and so on. Generally, cyclization effectively improves the specificity and stability of linear precursors [56, 57].

Transition metals such as iron, zinc, and copper can be chelated by proteins and play critical roles in the physiological activity of living subjects [58–60]. Rhenium (Re) and technetium (Tc) may share similar chemical properties and can be complexed with the chemical moieties in the side train of peptides, such as amide nitrogen, carboxylate oxygen, thiolate and thioether sulfur, resulting in the cyclized metallopeptide [52]. In the previous study, Giblin et al. firstly reported a Re–peptide complex named ReCCMSH (Fig. 1), which is cyclized of α -MSH analogs (CCMSH) through site-specific rhenium and technetium metal coordination, and these radiometallopeptides show significant improvement of

stability and affinity compared with linear CCMSH and excellent in vivo tumor imaging performance [52]. The tumor-targeting mechanism of ^{99m}Tc-CCMSH was further investigated and compared with ¹²⁵I-(Tyr²)-NDP, ^{99m}Tc-CGCG-NDP, ^{99m}Tc-Gly¹¹-CCMSH, and ^{99m}Tc-Nle¹¹-CCMSH [61]. Experimental results indicate that ^{99m}Tc-CCMSH shows high levels of cellular retention and tumor accumulation in murine melanoma mouse model with 6.55 ± 1.31 %ID/g in 4 h after injection. It is worth noting that ^{99m}Tc-CCMSH exhibits relative high uptake in the kidney. Interestingly, substitution of Lys¹¹ with Gly¹¹ or Nle¹¹ in the peptide probe can significantly reduce the kidney uptake, but the accumulation in tumor is also affected badly.

Following the above research, the macrocyclic chelate 1,4,7,10-tetraazacyclododecane-1,4,7,10-tetraacetic acid (DOTA) was introduced into the ReCCMSH, which can strongly chelate a variety of β and α radionuclides and expands the use of ReCCMSH peptide for PET/SPECT imaging and radionuclide therapy [62]. To investigate the effects of DOTA on tumor uptake and whole-body clearance, biodistributions of DOTA-ReCCMSH, ^{99m}Tc-CCMSH, disulfide bond-cyclized DOTA-CMSH, linear DOTA-CCMSH, and DOTA-NDP were compared in vivo. Among these tracers, ¹¹¹In-DOTA-ReCCMSH shows good tumor uptake, long time tumor tissue retention and rapid urine clearance [63]. Its molecular structure was further modified, and it revealed that substitution of Lys¹¹ with Arg¹¹ formed ¹¹¹In-6 can significantly increase tumor uptake and retention with equally good clearance rate as ¹¹¹In-DOTA-ReCCMSH [64]. Moreover, considering the advantages of halogen radionuclides, ReCCMSH was further modified and radiohalogenated by ¹²⁵I-iodobenzoate (¹²⁵I-IBA) resulting in Ac-dLys(¹²⁵I-IBA)-ReCCMSH(Arg¹¹). It exhibits comparable tumor uptake and retention properties with ¹¹¹In-DOTA-ReCCMSH in murine mice melanoma models, along with rapid clearance from the whole body through both urinary and gastrointestinal excretion [65].

Considering the high resolution of PET imaging and its widespread use in clinic, PET probes have been developed based on the α -MSH analogs investigated in previous studies. NAPamide as a representative of linear α -MSH analogs was radiolabeled with ⁶⁴Cu for PET imaging in vivo and visualization of the MC1R expression of murine/human melanoma mice models. ⁶⁴Cu-DOTA-NAPamide shows good tumor uptake value in B16F10 xenografted melanoma at 2 h post injection (4.63 ± 0.45 % ID/g), while the normal organs like liver and kidney also exhibit high accumulation and retention [66]. This phenomenon has also been observed for peptide-based probes in previous reported studies [54, 61, 64, 67, 68]. The high liver uptake is considered as the unstable radiocopper/DOTA complex. To reduce the uptake and retention in normal organs, N-succinimidyl-4-¹⁸F-fluorobenzoate (¹⁸F-SFB) was used to label NAPamide and

Table 1. Summary of the α -MSH analogs-based radioactive probes.

| Name | α -MSH analogs sequence | Radioisotope | Affinity (nM) | Injection time (h) | Tumor uptake (%ID/g) | Kidney uptake (%ID/g) | Reference(s) |
|---|---|-------------------|---|--------------------|----------------------|-----------------------|--------------|
| ^{99m} Tc-CCMSH | Ac- ^{99m} TcCEHdFRWCKPV-NH ₂ | ^{99m} Tc | 2.9 | 4 | 9.51 \pm 1.97 | 14.60 \pm 1.88 | [61] |
| ¹¹¹ In-DOTA-ReCCMSH | ¹¹¹ In-DOTA-ReCCEHdFRWCKPV-NH ₂ | ¹¹¹ In | 1.2 \pm 0.3 | 4 | 9.49 \pm 0.90 | 9.27 \pm 2.65 | [62] |
| ¹¹¹ In-6 | ¹¹¹ In-DOTA-ReCCEHdFRWCRPV-NH ₂ | ¹¹¹ In | 2.1 | 4 | 17.41 \pm 5.61 | 7.37 \pm 1.13 | [64] |
| Ac-D-Lys(¹²⁵ I-IBA)-ReCCMSH(Arg ¹¹) | Ac-dK(¹²⁵ I-IBA)-ReCCEHdFRWCRPV-NH ₂ | ¹²⁵ I | (2.08 \pm 0.04) \times 10 ⁻² | 4 | 15.10 \pm 1.38 | 8.57 \pm 0.87 | [65] |
| ⁶⁴ Cu-DOTA-NAPamide | Ac-NleDhFRWGK(DOTA- ⁶⁴ Cu)-NH ₂ | ⁶⁴ Cu | 3.66 \pm 0.29 | 2 | 4.63 \pm 0.45 | | [66] |
| ¹⁸ F-FB-NAPamide | Ac-NleDhFRWGK (¹⁸ F-FB)-NH ₂ | ¹⁸ F | 7.2 \pm 1.2 | 1 | 1.19 \pm 0.11 | 6.03 \pm 1.53 | [69] |
| ¹⁸ F-FB-RMSH-1 | Ac-dK(¹⁸ F-FB)ReCCEHdFRWCRPV-NH ₂ | ¹⁸ F | 5.4 \pm 0.7 | 2 | 2.11 \pm 0.12 | 5.42 \pm 0.50 | [70] |
| ¹⁸ F-FP-RMSH-1 | Ac-dK(¹⁸ F-FP)ReCCEHdFRWCRPV-NH ₂ | ¹⁸ F | 6.1 | 2 | 2.12 \pm 1.08 | 6.76 \pm 0.82 | [71] |

HdFRW is the critical sequence for MC1R.

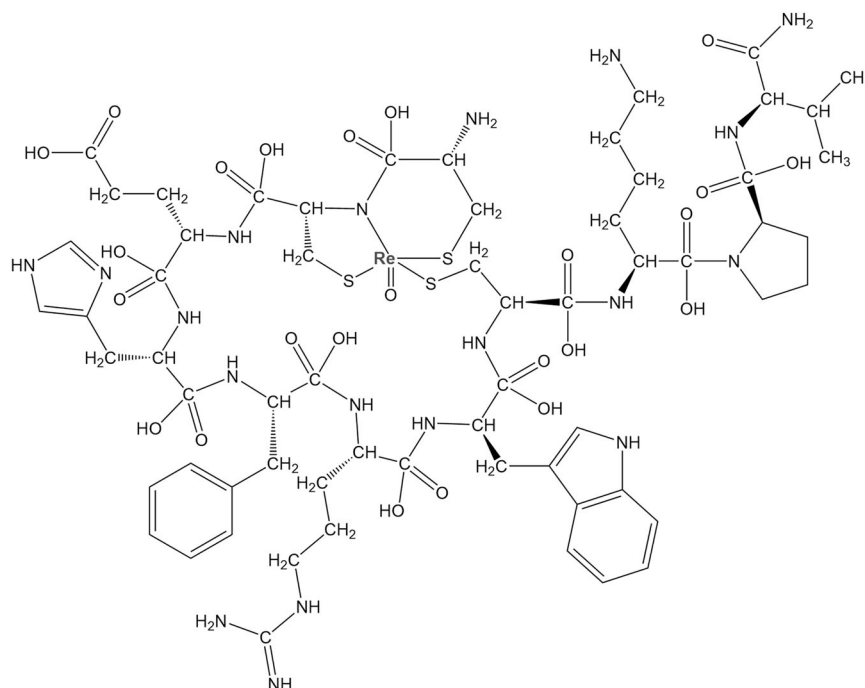


Fig. 1 Molecular structure of Ac-ReCCMSH-NH₂.

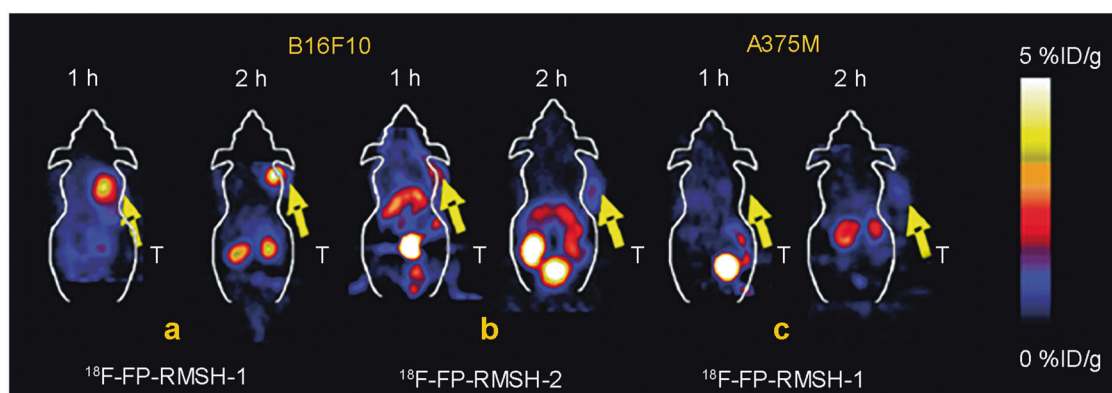


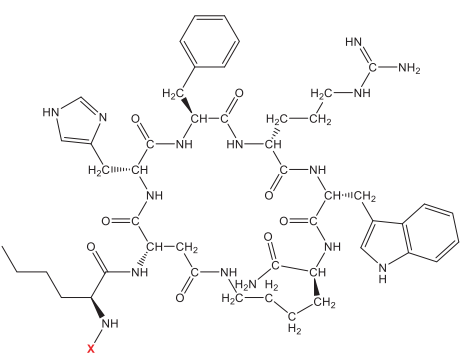
Fig. 2 PET images of ¹⁸F-FP-RMSH-1 and ¹⁸F-FP-RMSH-2 in vivo. Representative decay-corrected coronal small-animal PET images of mice-bearing B16F10 tumors on the right shoulder at 1 and 2 h after tail vein injections of ¹⁸F-FP-RMSH-1 **a** and -2 **b** ($n = 3$ for each group). T stands for tumor. **c** Representative decay-corrected coronal small-animal PET images of A375M tumor-bearing mice at indicated time points after a tail vein injection of ¹⁸F-FP-RMSH-1. Reprinted with permission from ref. [71].

generate ¹⁸F-FB-NAPamide. ¹⁸F-FB-NAPamide clearly demonstrates delineation of tumors. Compared with ⁶⁴Cu-DOTA-NAPamide, the uptake and retention of the liver, kidney along with B16F10 tumor tissues were reduced obviously [69]. Considering metalloprotein ReCCMSH exhibits better biodistribution profile than NAPamide in vivo, ¹⁸F-labeled ReCCMSH such as ¹⁸F-FB-RMSH-1/2 and ¹⁸F-FP-RMSH-1/2 were synthesized [70, 71]. ¹⁸F-FP-RMSH-1 displays equally good B16F10 tumor accumulation capacity with ¹⁸F-FB-RMSH-1 (5.4–6.1 %ID/g), while ¹⁸F-FP-RMSH-1 shows less uptake by liver because the improved hydrophilicity contributed by the use of 4-nitrophenyl 2-¹⁸F-fluoropropionate (¹⁸F-NFP). The PET images allow high tumor contrast for B16F10 but not A375M xenografted melanoma tumor model, because the expression level of MC1R in B16F10 is almost 18 times higher than that of A375M tumor (Fig. 2) [70]. The results illustrate that these MC1R-targeted molecular probes with good tumor uptake and retention have the potential to be used for imaging MC1R expression in clinic.

Furthermore, NAPamide analogs labeled with [^{99m}Tc(CO)₃]⁺ have been studied. Specifically, a cysteine residue is added to the terminal of NAPamide for complexing with the [M'(CO)₃]⁺ core and generating a potent tridentate chelate [72]. This cysteine-derived, N-S-N_{py} chelate [M'(CO)₃]⁺ core was first used to MC1R-targeted imaging, showing excellent radiolabeling yields and high stabilities both in vitro and in vivo. The radiolabeled peptide demonstrates rapid tumor accumulation as revealed through biodistribution and small-animal SPECT/CT studies. Then a novel chelate strategy based on the copper(I)-catalyzed azide-alkyne cycloaddition (CuAAC) click reaction with enhanced hydrophilicity has been developed and used with the *fac*-[M'(CO)₃]⁺ core [73]. The radiolabeling strategies explored in these studies can be used for generating a broad range of peptide-based targeted radiopharmaceuticals.

Besides metal-complexed α -MSH peptides, cyclized peptides based on lactam linkages also show high promise in peptides modification. Nle-CycMSHhex as one of the most classical lactam-

Table 2. Summary of the radioactive probes reported recently based on lactam cyclized of α -MSH analogs.

| X-Nle-CycMSH _{hex} | X | Model | Tumor Uptake (%ID/g) | Reference(s) |
|---|--|------------------------------|----------------------|--------------|
|  | ¹⁸ F-AmBF ₃ -Pip | B16/F10 Subcutaneous Tumor | 11.96 ± 2.31 (2 h) | [78] |
| | Al ¹⁸ F-NOTA -GG | B16/F10 Subcutaneous Tumor | 7.70 ± 1.71% (2 h) | [126] |
| | ⁹⁰ Y-DOTA-GG | B16/F10 Subcutaneous Tumor | 19.93 ± 5.73 (2 h) | [127] |
| | ²⁰³ Pb-DOTA-GG | B16/F-1 Subcutaneous Tumor | 12.61 ± 2.28 (2 h) | [128] |
| | | B16/F10 Subcutaneous Tumor | 16.81 ± 5.48 (2 h) | |
| | | B16/F10 Pulmonary Metastatic | 9.27 ± 1.13 (4 h) | |
| | ^{99m} Tc-(CO) ₃ -NOTA-GG | B16F10 Subcutaneous Tumor | 19.76 ± 3.62 (2 h) | [129] |
| | ⁶⁷ Ga-NODAGA-GG | B16F10 Subcutaneous Tumor | 14.96 ± 1.34 (2 h) | [130] |
| | ⁶⁴ Cu-NOTA-PEG ₂ | B16F10 Subcutaneous Tumor | 19.59 ± 1.48 (2 h) | [79] |
| | | | | |

cyclized α -MSH peptide has been carefully studied (Table 2). Various radiopharmaceuticals based on lactam-cyclized α -MSH peptide labeled with different radionuclides have been reported, such as ^{99m}Tc, ¹¹¹In, ⁶⁷Ga, and ⁶⁴Cu [74–76]. Impressively, ⁶⁸Ga-DOTA-GGNle-CycMSH_{hex} was firstly evaluated in two melanoma patients for visualization of metastases melanoma lesions in 2018. Compared with ¹⁸F-FDG PET/CT, images of ⁶⁸Ga-DOTA-GGNle-CycMSH_{hex} represent the expression level of MC1R in different metastases foci [77].

Considering the outstanding performance of ⁶⁸Ga-DOTA-GGNle-CycMSH_{hex} in clinical studies, in the following years, several novel radiotracers were reported and showed high potential in clinical applications (Table 2). Zhang et al. reported three ¹⁸F-labeled Nle-CycMSH_{hex} peptides with different linkers and evaluated their tumor uptake and biodistribution properties in B16F10 murine tumor models. Among these probes, CCZ01064 with 4-amino-(1-carboxymethyl) piperidine (Pip) linker (AmBF₃-Pip) shows the highest tumor accumulation and equally low uptake in normal organs [78]. ⁶⁴Cu is another widely used radioisotope in PET. In the previous studies, Guo et al. have demonstrated that ⁶⁴Cu-NOTA-GGNle-CycMSH_{hex} exhibits better tumor-specific imaging performance than ⁶⁴Cu-DOTA-GGNle-CycMSH_{hex} [76]. Recently, Qiao et al. further investigated the linker between the NOTA and CycMSH_{hex}. Compared to ⁶⁴Cu-NOTA-AocNle-CycMSH_{hex}, ⁶⁴Cu-NOTA-PEG₂Nle-CycMSH_{hex} shows higher tumor uptake, tumor/kidney ratio and tumor/liver ratio [79]. These studies highlight that radiolabeling of Nle-CycMSH_{hex} for melanoma-specific imaging is an important strategy and shows high potential for clinical translation.

Moreover, these imaging probes can be transformed into therapeutic radiopharmaceuticals, through radiolabeling with beta-radionuclide or alpha-emitter such as radiohalogenation (¹³¹I), radiometal (¹⁷⁷Lu, ⁹⁰Y, ²¹²Pb, etc.). Several reviews have been published and introduce the radionuclide therapy agents for MC1R [49, 80–82].

MELANIN-ASSOCIATED RADIOTRACERS

Melanin is a biopolymer made up of eumelanin and pheomelanin, which mainly present in the skins and are responsible for the pigmentation of the hair, eyes, and mucosa. Melanin pigments are synthesized by melanosomes which locate inside melanocytes and melanoma cells, then they are transferred into the surrounding keratinocytes. Melanin plays an essential role in protecting the cells against ultraviolet radiation damage and oxidative stress [83–87].

Most of the primary cutaneous melanoma and metastatic melanoma tumors contain pigmentation of melanin granule, only

1.8%–8.1% are amelanotic [88, 89]. Melanin targeting compounds can thus serve as molecular platform for developing melanoma-specific imaging probes. It should also be noted that melanin pigment is considered as a double-edge sword as revealed by some research, because it may also accelerate melanoma's progression and make melanoma cells resistant to different types of treatment [90, 91]. Overall, melanin is a promising biomarker for melanoma diagnosis and therapy, and a variety of radiopharmaceuticals have been developed for melanoma SPECT and PET imaging. In the last decade, melanin-targeted PET probes have been actively pursued and some important advancements have been achieved in preclinical and clinical studies.

MELANIN-TARGETED SMALL-MOLECULE-BASED PROBES

Various small molecules have been found to bind to melanin both in vivo and in vitro. All these molecules contain an aromatic or heteroaromatic ring and a protonated amine function at physiological pH, such as methylene blue (MTB), chlorpromazine, adifenine, chloroquine, acridine orange, benzamide (BZA) and its analogs [50, 87, 92, 93]. The N-(2-diethylaminoethyl)-4-iodobenzamide (BZA) was first found to accumulate in melanoid structures and can be used for malignant melanoma imaging in 1991 [94]. Since then several ¹²³I/¹²⁵I labeled BZA analogs have been developed for melanoma planar scintigraphy or SPECT imaging [94]. Some of these radiotracers such as ¹²³I-BZA and ¹²³I-BZA₂ were evaluated in malignant melanoma patients, and the results indicate the capacity of these radiopharmaceuticals to discriminate between benign and malignant lesions [95, 96]. However, compared with ¹⁸F-FDG PET, ¹²³I-BZA₂ shows decreased sensitivity and lower accuracy for the diagnosis of melanin-positive metastatic melanoma [97]. The development of benzamide-based PET probes becomes a promising strategy for diagnosis of malignant primary and metastasis melanoma, and numerous probes have been reported (Table 3).

In 2009, the development of N-[2-(diethylamino) ethyl]-4-¹⁸F-fluorobenzamide (¹⁸F-FBZA) was reported to image both primary and lung metastasis of malignant melanoma [98]. ¹⁸F-FBZA shows high B16F10 tumor uptake in subcutaneous melanoma tumors (5.94 ± 1.83 %ID/g) at 2 h after injection, but very low uptake in amelanotic A375M (0.75 ± 0.09 %ID/g) and U87MG (0.56 ± 0.13 %ID/g) tumors. For B16F10 pulmonary metastasis model, microPET imaging clearly shows a region of uptake in the thoracic cavity, but low signals are detected in the normal lung tissue (Fig. 3a). The biodistribution study confirms that much higher ¹⁸F-FBZA accumulation in melanoma lung

Table 3. Summary of melanin-targeted radiotracers.

| Structure | Name | Radiosynthesis time | Radiochemical yield | Purification | Chemical precursor | Molar activity | Reference(s) |
|-----------|--|---------------------|---------------------|--------------|--------------------|---------------------|--------------|
| | ¹⁸ F-FBZA/ ¹⁸ F-DAFBA | 3 h | 50% | 95% | | 132–166 GBq/mmol | [98, 131] |
| | ¹⁸ F-1 | <1 h | 24.5% ± 6.7% | >95% | | 100–150 GBq/μmol | [101] |
| | ¹⁸ F-2/ ¹⁸ F-P3BZA | <1 h | 9.5% ± 1.9% | >95% | | 100–150 GBq/μmol | [101] |
| | ¹⁸ F-3/ ¹⁸ F-MEL050 | <1 h | 21.5% ± 15.5% | >95% | | 100–150 GBq/μmol | [99–101] |
| | ¹⁸ F-FPDA | 30 min | 79.8% | >99% | | — | [104] |

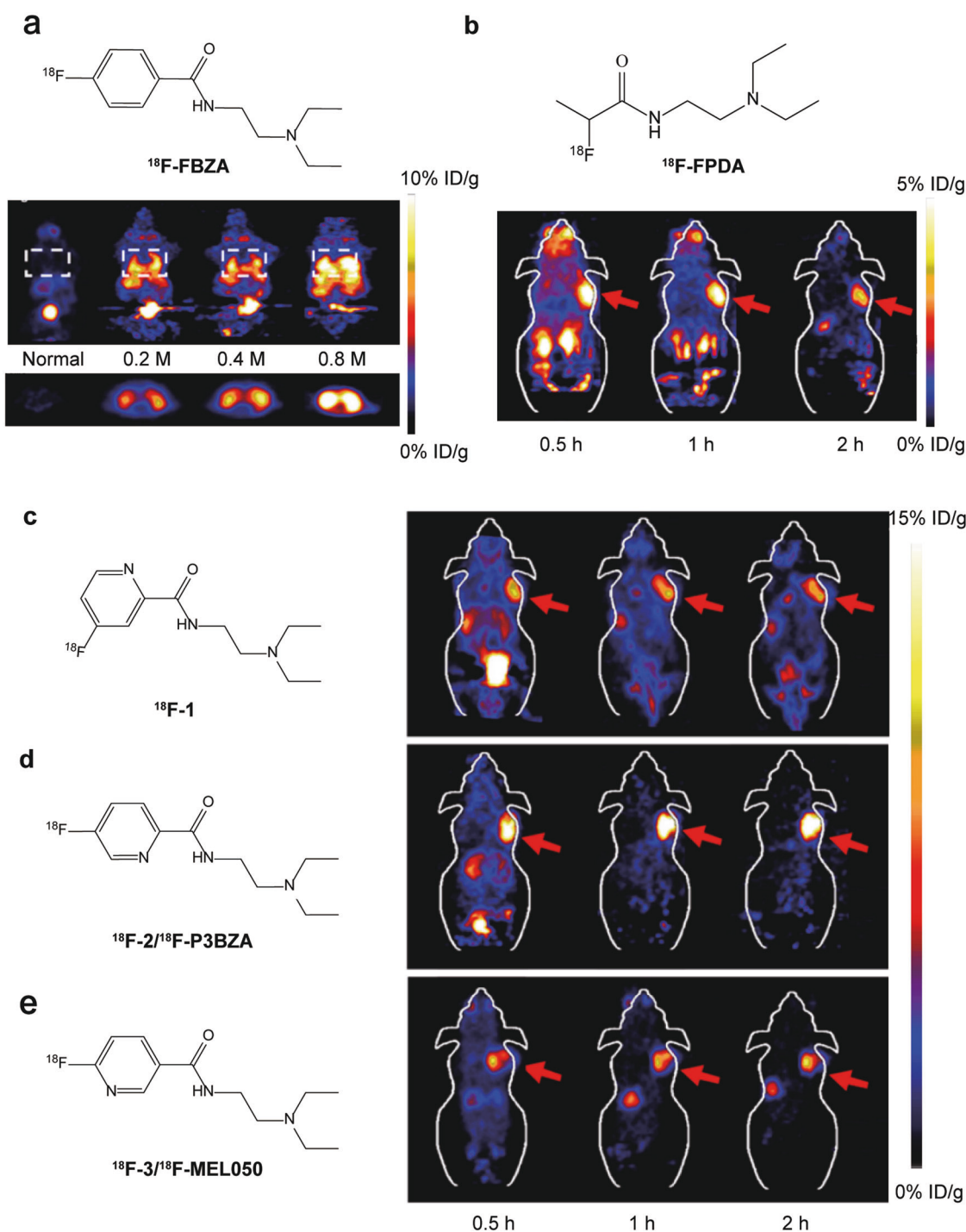


Fig. 3 Molecular structures of the probes and PET images of melanoma tumor models. **a** Representative decay-corrected coronal (top) and transaxial (bottom) small-animal PET images of B16F10 melanoma lung metastasis model that was established 13 d after tail vein injection of 0.2×10^6 ($n = 3$), 0.4×10^6 ($n = 3$), or 0.8×10^6 ($n = 2$) B16F10 cells. **b** Decay-corrected whole-body coronal PET images of mice bearing B16F10 tumors from static scans at 0.5, 1, and 2 h after the injection of ^{18}F -FPDA. The tumors are indicated with red arrows. **c–e** Decay-corrected whole-body coronal small animal PET images of C57BL/6 mice bearing B16F10 murine melanomas from a static scan at 0.5, 1, and 2 h after injection of ^{18}F -1, ^{18}F -2 (^{18}F -P3BZA) and ^{18}F -3. Tumors are indicated by red arrows. Adapted with permission from refs. [98, 101, 104].

metastases (7.87 ± 3.56 %ID/g) than that of normal lung tissue (0.99 ± 0.04 %ID/g).

However, the radiosynthesis of ^{18}F -FBZA needs multiple steps up to 3 h which significantly limits its production and applications in the clinic. To solve this problem, Greguric et al. report a series of ^{18}F -fluoronicotinamide radiotracers prepared in one simple radio-synthetic step within 40 min [99], and one of them, [^{18}F]N-(2-

(diethylamino)ethyl)-6-fluoronicotinamide (^{18}F -3/ ^{18}F -MEL050) shows melanin-specific accumulation and high tumor retention [100]. Based on its advantages in radiosynthesis and performance in vivo, more ^{18}F -MEL050 analogs including N-(2-(diethylamino)ethyl)- ^{18}F -4-fluoropicolinamide (^{18}F -1) and N-(2-(diethylamino)ethyl)- ^{18}F -5-fluoropicolinamide (^{18}F -2) were designed and biologically evaluated in small-animal models (Fig. 3c–e) [101]. Small-animal PET imaging

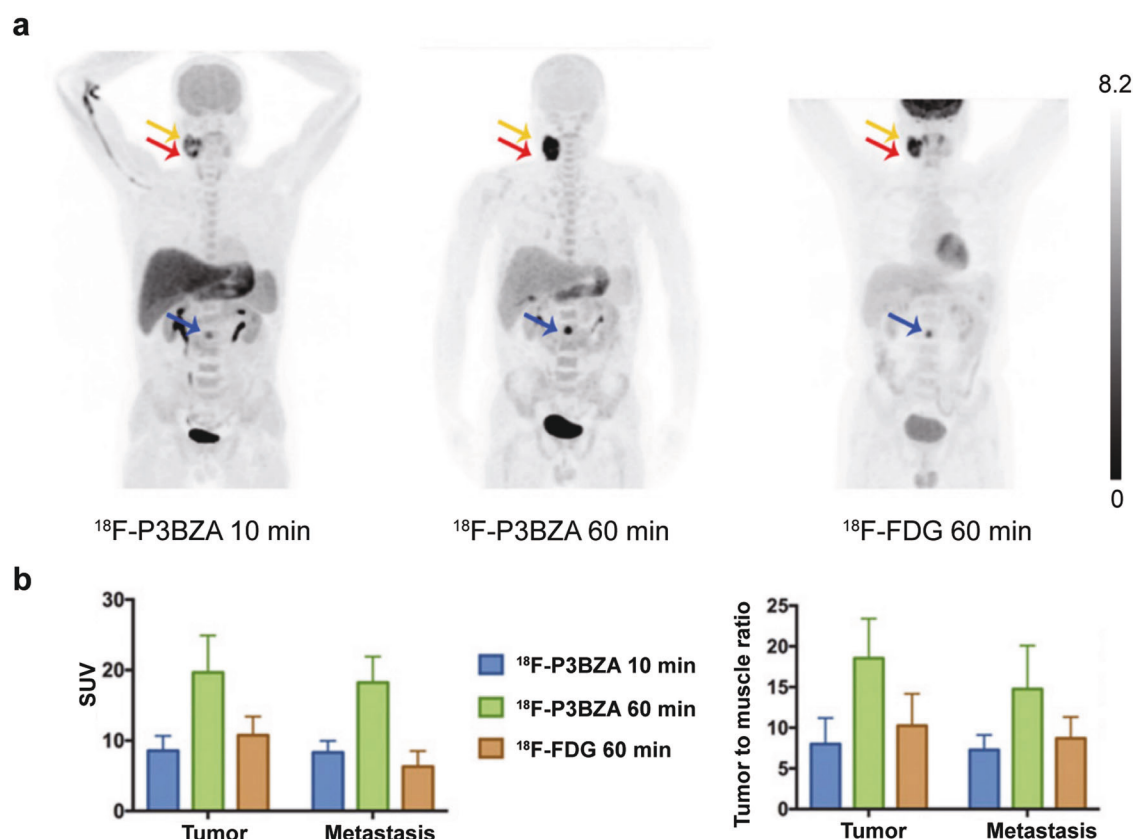


Fig. 4 The performance of ^{18}F -P3BZA in melanoma patients. **a** Maximum-intensity-projection PET images of one melanoma patient at 10 and 60 min after ^{18}F -P3BZA injection and at 60 min after ^{18}F -FDG injection. **b** Average SUV_{mean} and tumor-to-muscle ratio of melanoma tumors and metastases in patients ($n = 5$). Adapted with permission from ref. [106].

and biodistribution studies indicate all these PET probes with melanin-targeted capacity exhibit excellent tumor imaging contrasts and favorable biodistribution patterns. Particularly ^{18}F -2 shows the highest tumor uptake of 16.87 ± 1.23 %ID/g at 2 h, while ^{18}F -1 and ^{18}F -3 are 9.73 ± 1.41 %ID/g and 8.47 ± 1.35 %ID/g, respectively. Moreover, ^{18}F -2 shows the highest tumor-to-muscle ratios (36.79 ± 5.21) than those of ^{18}F -1 and ^{18}F -3 ($P < 0.05$). ^{18}F -2 is identified as an excellent candidate for translation into clinical PET imaging melanoma. Besides melanoma-specific targeted imaging, ^{18}F -2 also can serve as PET probe for imaging of human tyrosinase (TYR) gene expression and tracking of porcine retinal pigment epithelium (prPE) cells in vivo [102, 103].

To reduce the probe uptake in liver, the aromatic ring structure was removed from benzamide molecular scaffold, and a novel melanin binding radiotracer N-(2-(diethylamino)ethyl)-2- ^{18}F -fluoropropanamide (^{18}F -FPDA) was synthesized (Fig. 3b) [104]. Compared to ^{18}F -1/2/3, ^{18}F -FPDA shows lower lipophilicity and liver uptake is only 1.39 ± 0.11 %ID/g at 1 h post injection. At the same time, the melanotic melanoma targeting ability of ^{18}F -FPDA (5.41 ± 1.47 % ID/g at 0.5 h) was found to be reduced because of lacking the aromatic ring.

Based on the radiosynthesis procedure, melanin-specific targeting ability, and biodistribution profile of these radiotracers, ^{18}F -P3BZA shows high potential for clinical application, thus it was selected for further study in humans. Six healthy volunteers and 5 patients with suspected melanomas were imaged with ^{18}F -P3BZA. This pilot clinical study demonstrates that the imaging dose of ^{18}F -P3BZA is safe and tolerable. ^{18}F -FDG as a comparison was also performed 3 days after ^{18}F -P3BZA PET/CT imaging for the patients enrolled. The results indicate that ^{18}F -P3BZA distributes to the melanoma quickly in 10 min and shows tumor tissues with high contrast. Both ^{18}F -P3BZA and ^{18}F -FDG PET/CT can detect primary

melanomas with the average SUV_{max} 19.7 ± 5.3 and 10.8 ± 2.7 , respectively. For metastases lesions including 2 lymph node metastases and 1 bone metastasis, the average SUV_{max} of ^{18}F -P3BZA and ^{18}F -FDG PET/CT is 18.2 ± 3.7 and 6.3 ± 2.2 , respectively (Fig. 4) [105]. This first-in-human clinical application of ^{18}F -P3BZA to melanoma demonstrates its potential for malignant melanoma PET/CT imaging.

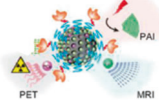
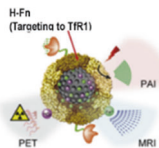
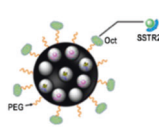
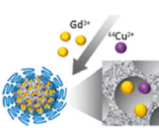
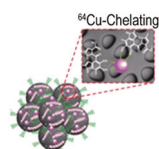
The synthesis procedure of ^{18}F -P3BZA was further optimized by investigating a solid-phase extraction-based method for purification. The automated radiosynthesis process for producing high radioactivity and high purity of ^{18}F -P3BZA can be completed within 40 min. This convenient and efficient purification method for ^{18}F -P3BZA can be applied in different scenarios, promoting the broad use of ^{18}F -P3BZA [106].

Pyo et al. reported a novel benzamide derivative [^{18}F]DMFB based on ^{18}F -FPDA with shortened from diethyl to dimethyl [107]. Compared with ^{18}F -FDG and ^{18}F -P3BZA, [^{18}F]DMFB showed high accumulation in B16F10 xenografts (24.8% %ID/g, 1 h) and better tumor-to-background contrast. Moreover, [^{18}F]DMFB allowed clear-cut visualization of metastasis lesions in the lungs and lymph nodes. The melanin-targeted probe [^{18}F]DMFB is a promising candidate for both primary and metastasis melanoma diagnosis in clinics. Recently, Xiaoli Lan's team further studied the melanin-specific tracer ^{18}F -PFPN with melanoma patients, which can visualize the metastases of melanoma successfully [108, 109].

MELANIN-BASED PROBES FOR MOLECULAR IMAGING APPLICATIONS

Melanin has been traditionally used as a melanoma biomarker, and numerous melanin-targeted imaging and therapeutic agents have been developed. Interestingly, because of the polymeric

Table 4. Summary of melanin-based nanoparticles and their biomedical applications.

| Nanoparticles | Illustration | Size | Target | Imaging modalities | Radionuclide | Therapeutic strategies | Reference(s) |
|--------------------------------------|--|----------|---------------------------------|--------------------|------------------|------------------------|--------------|
| RGD-functionalized PEG-MNP |  | ~9.6 nm | $\alpha v \beta 3$ integrins | PET/MRI/PAI | ^{64}Cu | | [110] |
| AMF |  | ~16.4 nm | transferrin receptor 1 | PET/MRI/PAI | ^{64}Cu | | [111] |
| (^{124}I , Mn) OCT-PEG-MNP |  | ~13.8 nm | Somatostatin receptor subtype 2 | PET/MRI/PAI | ^{124}I | | [114] |
| M-dots |  | ~15 nm | | PET/MRI/PAI | ^{64}Cu | | [113] |
| SRF-MNP |  | ~60.0 nm | | PET/MRI/PAI | ^{64}Cu | Sorafenib | [112] |

Adapted with permission from refs. [110–114].

nature and high biocompatibility of melanin, it can also serve as a novel biomaterial platform for developing agents for diverse biomedical applications such as multimodal imaging and theranostics. In 2014, our team demonstrated the synthesis of ultra-small water-soluble melanin nanoparticles (PEG-MNPs) and further modified it with biomolecule such as RGD peptide (RGD-PEG-MNPs) for PET/PAI/MRI multimodal imaging of other type of tumor beyond melanoma [110]. The RGD-PEG-MNPs can easily bind with ^{64}Cu and Fe^{3+} ions to realize PET and MR imaging capability without surface modification and introducing chelating groups, because of the natural metal ions binding capacity of melanin. The results indicate that the nanoparticles show good in vivo tumor imaging properties, and the multimodal imaging strategies combine the advantages of each imaging modality and may overcome the limitations of individuals. Subsequently, we and other groups further developed many melanin-based nanoparticles with attractive tumor imaging and therapy properties (some of the work are shown in Table 4) [111–116]. Xia et al. reported a novel melanin nanoprobe (PMNs-II-813) which coupled with PSMA (prostate-specific membrane antigen) inhibitor for prostate cancer targeted theranostics. The nanoprobe can stably complex with ^{89}Zr and Mn^{2+} for PET and MRI multimodal diagnosis. It also demonstrated radioisotope therapy (RIT) and PTT capability after labeled with a therapeutic radionuclide, ^{131}I , and showed inhibitory effect on prostate cancer growth [117]. Recently Zhang et al. developed a nanodrug delivery platform for

rhabdomyolysis-induced acute kidney injury (AKI) treatment based on melanin nanoparticles, which could effectively reduce oxidative stress, apoptosis, and inflammatory response in mice AKI models [118].

This work highlights that melanin as a natural biopolymer with excellent biocompatibility shows a novel and attractive strategy for the formulation of multifunctional nanoparticles for various biomedical applications. It also represents the success of transferring a tumor biomarker into a theranostic platform. In addition, polydopamine as a melanin mimetic material also shows promising potential in various fields' studies, and several reviews have been published in recent years [119–125].

CONCLUSION

The development of novel, sensitive, and specific radiotracers for melanoma with high potential to overcome the limitations of ^{18}F -FDG remains a goal in the molecular imaging community. Various target ligands have been investigated, including small molecules, peptides, monoclonal antibodies, nanoparticles, etc. These molecules demonstrate different pharmacokinetics. Their advantages and disadvantages are two sides of the same coin and can transform in different situations. It is not realistic to rely on one type of molecular platform for probe development for all diseases. To promote the development of molecular imaging, all types of molecular platforms can be explored to identify the best

approach, including nanoparticles that can be used for multimodal imaging on different scales at the same time.

In this review, molecular probes targeting to the MC1R and melanin in melanoma have been demonstrated to be promising and valid melanoma theranostics strategies. A plethora of radiotracers with outstanding tumor targeting and in vivo biodistribution properties have been developed, and some of them have shown outstanding imaging properties in melanoma patients as well. Further studies could possibly be focused on applying the radiotracers to more clinical translation studies and developing more radiopharmaceuticals for both visualization and treatment of melanoma patients.

ACKNOWLEDGEMENTS

The authors thank funding from the Shanghai Municipal Science and Technology Major Project.

ADDITIONAL INFORMATION

Competing interests: The authors declare no competing interests.

REFERENCES

- Cancer stat facts: melanoma of the skin. 2019. <https://seer.cancer.gov/statfacts/html/melan.html>.
- Gershenwald JE, Guy GP Jr. Stemming the rising incidence of melanoma: calling prevention to action. *J Natl Cancer Inst*. 2016;108:djv381.
- Karimkhani C, Green AC, Nijsten T, Weinstock MA, Dellavalle RP, Naghavi M, et al. The global burden of melanoma: results from the Global Burden of Disease Study 2015. *Br J Dermatol*. 2017;177:134–40.
- Schadendorf D, van Akkooi ACJ, Berking C, Griewank KG, Gutzmer R, Hauschild A, et al. Melanoma. *Lancet*. 2018;392:971–84.
- Carr S, Smith C, Wernberg J. Epidemiology and risk factors of melanoma. *Surg Clin North Am*. 2020;100:1–12.
- Lincoff E, Swetter SM, Cockburn MG, Colditz GA, Clarke CA. Increasing burden of melanoma in the United States. *J Invest Dermatol*. 2009;129:1666–74.
- Guy GP Jr., Thomas CC, Thompson T, Watson M, Massetti GM, Richardson LC, et al. Vital signs: melanoma incidence and mortality trends and projections—United States, 1982–2030. *MMWR Morb Mortal Wkly Rep*. 2015;64:591–6.
- Whiteman DC, Green AC, Olsen CM. The growing burden of invasive melanoma: projections of incidence rates and numbers of new cases in six susceptible populations through 2031. *J Invest Dermatol*. 2016;136:1161–71.
- Welch HG, Mazer BL, Adamson AS. The rapid rise in cutaneous melanoma diagnoses. *N Engl J Med*. 2021;384:72–9.
- Joyce D, Skitzki JJ. Surgical management of primary cutaneous melanoma. *Surg Clin North Am*. 2020;100:61–70.
- Survival rates for melanoma skin cancer. 2022. <https://www.cancer.org/cancer/melanoma-skin-cancer/detection-diagnosis-staging/survival-rates-for-melanoma-skin-cancer-by-stage.html>.
- Singh AD, Topham A. Survival rates with uveal melanoma in the United States: 1973–1997. *Ophthalmology*. 2003;110:962–5.
- Brozyna AA, Jozwicki W, Carlson JA, Slominski AT. Melanogenesis affects overall and disease-free survival in patients with stage III and IV melanoma. *Hum Pathol*. 2013;44:2071–4.
- Abbasi NR, Shaw HM, Rigel DS, Friedman RJ, McCarthy WH, Osman I, et al. Early diagnosis of cutaneous melanoma: revisiting the ABCD criteria. *J Am Med Assoc*. 2004;292:2771–6.
- Rigel DS, Russak J, Friedman R. The evolution of melanoma diagnosis: 25 years beyond the ABCDs. *CA Cancer J Clin*. 2010;60:301–16.
- Tatro JB, Atkins M, Mier JW, Hardarson S, Wolfe H, Smith T, et al. Melanotropin receptors demonstrated in situ in human melanoma. *J Clin Invest*. 1990;85:1825–32.
- Breslow A. Thickness, cross-sectional areas and depth of invasion in the prognosis of cutaneous melanoma. *Ann Surg*. 1970;172:902–8.
- Scolyer RA, Long GV, Thompson JF. Evolving concepts in melanoma classification and their relevance to multidisciplinary melanoma patient care. *Mol Oncol*. 2011;5:124–36.
- Lee C, Collichio F, Ollila D, Moschos S. Historical review of melanoma treatment and outcomes. *Clin Dermatol*. 2013;31:141–7.
- Rebecca VW, Sondak VK, Smalley KS. A brief history of melanoma: from mummies to mutations. *Melanoma Res*. 2012;22:114–22.
- Belhocine TZ, Scott AM, Even-Sapir E, Urbain JL, Essner R. Role of nuclear medicine in the management of cutaneous malignant melanoma. *J Nucl Med*. 2006;47:957–67.
- Dancey AL, Mahon BS, Rayatt SS. A review of diagnostic imaging in melanoma. *J Plast Reconstr Aesthet Surg*. 2008;61:1275–83.
- Davis LE, Shalin SC, Tackett AJ. Current state of melanoma diagnosis and treatment. *Cancer Biol Ther*. 2019;20:1366–79.
- Perissinotti A, Rietbergen DD, Vidal-Sicart S, Riera AA, Olmos RAV. Melanoma & nuclear medicine: new insights & advances. *Melanoma Manag*. 2018;5:MMT06.
- Schwimmer J, Essner R, Patel A, Jahan SA, Shepherd JE, Park K, et al. A review of the literature for whole-body FDG PET in the management of patients with melanoma. *Q J Nucl Med*. 2000;44:153–67.
- Crippa F, Leutner M, Belli F, Gallino F, Greco M, Pilotti S, et al. Which kinds of lymph node metastases can FDG PET detect? A clinical study in melanoma. *J Nucl Med*. 2000;41:1491–4.
- Ghanem N, Althoefer C, Hoyerle S, Nitzsche E, Lohmann C, Schafer O, et al. Detectability of liver metastases in malignant melanoma: prospective comparison of magnetic resonance imaging and positron emission tomography. *Eur J Radiol*. 2005;54:264–70.
- Vercellino L, de Jong D, Dercle L, Hosten B, Braumüller B, Das JP, et al. Translating molecules into imaging—the development of new PET tracers for patients with melanoma. *Diagnostics*. 2022;12:1116.
- Annunziata S, Laudicella R, Caobelli F, Pizzuto DA, Aimn Working Group Y. Clinical value of PET/CT in staging melanoma and potential new radiotracers. *Curr Radiopharm*. 2020;13:6–13.
- Holcomb NC, Bautista RM, Jarrett SG, Carter KM, Gober MK, D'Orazio JA. cAMP-mediated regulation of melanocyte genomic instability: a melanoma-preventive strategy. *Adv Protein Chem Struct Biol*. 2019;115:247–95.
- Wolf Horrell EM, Boulanger MC, D'Orazio JA. Melanocortin 1 receptor: structure, function, and regulation. *Front Genet*. 2016;7:95.
- Landi MT, Bauer J, Pfeiffer RM, Elder DE, Hulley B, Minghetti P, et al. MC1R germline variants confer risk for BRAF-mutant melanoma. *Science*. 2006;313:521–2.
- Raimondi S, Sera F, Gandini S, Iodice S, Caini S, Maisonneuve P, et al. MC1R variants, melanoma and red hair color phenotype: a meta-analysis. *Int J Cancer*. 2008;122:2753–60.
- Fargnoli MC, Gandini S, Peris K, Maisonneuve P, Raimondi S. MC1R variants increase melanoma risk in families with CDKN2A mutations: a meta-analysis. *Eur J Cancer*. 2010;46:1413–20.
- Kanetsky PA, Panossian S, Elder DE, Guerry D, Ming ME, Schuchter L, et al. Does MC1R genotype convey information about melanoma risk beyond risk phenotypes? *Cancer*. 2010;116:2416–28.
- Punertvoll HE, Yang XR, Vetti HH, Bachmann IM, Avril MF, Benfodda M, et al. Melanoma prone families with CDK4 germline mutation: phenotypic profile and associations with MC1R variants. *J Med Genet*. 2013;50:264–70.
- Pasquali E, Garcia-Borrón JC, Fargnoli MC, Gandini S, Maisonneuve P, Bagnardi V, et al. MC1R variants increased the risk of sporadic cutaneous melanoma in darker-pigmented Caucasians: a pooled-analysis from the M-SKIP project. *Int J Cancer*. 2015;136:618–31.
- Swope VB, Jameson JA, McFarland KL, Supp DM, Miller WE, McGraw DW, et al. Defining MC1R regulation in human melanocytes by its agonist alpha-melanocortin and antagonists agouti signaling protein and beta-defensin 3. *J Invest Dermatol*. 2012;132:2255–62.
- Rosenkranz AA, Slasnikova TA, Durymanov MO, Sobolev AS. Malignant melanoma and melanocortin 1 receptor. *Biochemistry*. 2013;78:1228–37.
- Salazar-Onfray F, Lopez M, Lundqvist A, Aguirre A, Escobar A, Serrano A, et al. Tissue distribution and differential expression of melanocortin 1 receptor, a malignant melanoma marker. *Br J Cancer*. 2002;87:414–22.
- Catania A, Lipton JM. alpha-Melanocyte stimulating hormone in the modulation of host reactions. *Endocr Rev*. 1993;14:564–76.
- Miller R, Aaron W, Toneff T, Vishnuvardhan D, Beinfeld MC, Hook VY. Obliteration of alpha-melanocyte-stimulating hormone derived from POMC in pituitary and brains of PC2-deficient mice. *J Neurochem*. 2003;86:556–63.
- Bagutti C, Stolz B, Albert R, Bruns C, Pless J, Eberle AN. [¹¹¹In]-DTPA-labeled analogues of alpha-melanocyte-stimulating hormone for melanoma targeting: receptor binding in vitro and in vivo. *Int J Cancer*. 1994;58:749–55.
- Cowell SM, Balse-Srinivasan PM, Ahn JM, Hruby VJ. Design and synthesis of peptide antagonists and inverse agonists for G protein-coupled receptors. *Methods Enzymol*. 2002;343:49–72.
- Raposo PD, Correia JD, Oliveira MC, Santos I. Melanocortin-1 receptor-targeting with radiolabeled cyclic alpha-melanocyte-stimulating hormone analogs for melanoma imaging. *Biopolymers*. 2010;94:820–9.
- Hruby VJ, Cai M, Grieco P, Han G, Kavarana M, Trivedi D. Exploring the stereostructural requirements of peptide ligands for the melanocortin receptors. *Ann N Y Acad Sci*. 2003;994:12–20.

47. Abdel-Malek ZA, Ruwe A, Kavanagh-Starnier R, Kadekaro AL, Swope V, Haskell-Luevano C, et al. alpha-MSH tripeptide analogs activate the melanocortin 1 receptor and reduce UV-induced DNA damage in human melanocytes. *Pigment Cell Melanoma Res.* 2009;22:635–44.
48. Heppeler A, Froidevaux S, Eberle AN, Maecke HR. Receptor targeting for tumor localisation and therapy with radiopeptides. *Curr Med Chem.* 2000;7:971–94.
49. Quinn T, Zhang X, Miao Y. Targeted melanoma imaging and therapy with radiolabeled alpha-melanocyte stimulating hormone peptide analogues. *G Ital Dermatol Venereol.* 2010;145:245–58.
50. Wei W, Ehlerding EB, Lan X, Luo Q, Cai W. PET and SPECT imaging of melanoma: the state of the art. *Eur J Nucl Med Mol Imaging.* 2018;45:132–50.
51. Sawyer TK, Sanfilippo PJ, Hruby VJ, Engel MH, Heward CB, Burnett JB, et al. 4-Norleucine, 7-D-phenylalanine-alpha-melanocyte-stimulating hormone: a highly potent alpha-melanotropin with ultralong biological activity. *Proc Natl Acad Sci USA.* 1980;77:5754–8.
52. Giblin MF, Wang N, Hoffman TJ, Jurisson SS, Quinn TP. Design and characterization of alpha-melanotropin peptide analogs cyclized through rhenium and technetium metal coordination. *Proc Natl Acad Sci USA.* 1998;95:12814–8.
53. Froidevaux S, Calame-Christe M, Schuhmacher J, Tanner H, Saffrich R, Henze M, et al. A gallium-labeled DOTA-alpha-melanocyte-stimulating hormone analog for PET imaging of melanoma metastases. *J Nucl Med.* 2004;45:116–23.
54. Froidevaux S, Calame-Christe M, Tanner H, Eberle AN. Melanoma targeting with DOTA-alpha-melanocyte-stimulating hormone analogs: structural parameters affecting tumor uptake and kidney uptake. *J Nucl Med.* 2005;46:887–95.
55. Yang Y, Dickinson C, Haskell-Luevano C, Gantz I. Molecular basis for the interaction of [Nle4,D-Phe7]melanocyte stimulating hormone with the human melanocortin-1 receptor. *J Biol Chem.* 1997;272:23000–10.
56. Roxin A, Zheng G. Flexible or fixed: a comparative review of linear and cyclic cancer-targeting peptides. *Future Med Chem.* 2012;4:1601–18.
57. Conibear AC, Chaousis S, Durek T, Rosengren KJ, Craik DJ, Schroeder CI. Approaches to the stabilization of bioactive epitopes by grafting and peptide cyclization. *Biopolymers.* 2016;106:89–100.
58. Klemba M, Gardner KH, Marino S, Clarke ND, Regan L. Novel metal-binding proteins by design. *Nat Struct Biol.* 1995;2:368–73.
59. Lau SJ, Laussac JP, Sarkar B. Synthesis and copper(II)-binding properties of the N-terminal peptide of human alpha-fetoprotein. *Biochem J.* 1989;257:745–50.
60. Franco R, Moura JJ, Moura I, Lloyd SG, Huynh BH, Forbes WS, et al. Characterization of the iron-binding site in mammalian ferroxidase by kinetic and Mossbauer methods. *J Biol Chem.* 1995;270:26352–7.
61. Chen J, Cheng Z, Hoffman TJ, Jurisson SS, Quinn TP. Melanoma-targeting properties of ^{99m}Tc-labeled cyclic alpha-melanocyte-stimulating hormone peptide analogues. *Cancer Res.* 2000;60:5649–58.
62. Chen J, Cheng Z, Owen NK, Hoffman TJ, Miao Y, Jurisson SS, et al. Evaluation of an ¹¹¹In-DOTA-rhenium cyclized alpha-MSH analog: a novel cyclic-peptide analog with improved tumor-targeting properties. *J Nucl Med.* 2001;42:1847–55.
63. Chen J, Cheng Z, Miao Y, Jurisson SS, Quinn TP. Alpha-melanocyte-stimulating hormone peptide analogs labeled with technetium-99m and indium-111 for malignant melanoma targeting. *Cancer.* 2002;94:1196–201.
64. Cheng Z, Chen J, Miao Y, Owen NK, Quinn TP, Jurisson SS. Modification of the structure of a metalloprotein: synthesis and biological evaluation of ¹¹¹In-labeled DOTA-conjugated rhenium-cyclized alpha-MSH analogues. *J Med Chem.* 2002;45:3048–56.
65. Cheng Z, Chen J, Quinn TP, Jurisson SS. Radioiodination of rhenium cyclized alpha-melanocyte-stimulating hormone resulting in enhanced radioactivity localization and retention in melanoma. *Cancer Res.* 2004;64:1411–8.
66. Cheng Z, Xiong Z, Subbarayan M, Chen X, Gambhir SS. ⁶⁴Cu-labeled alpha-melanocyte-stimulating hormone analog for microPET imaging of melanocortin 1 receptor expression. *Bioconjug Chem.* 2007;18:765–72.
67. McQuade P, Miao Y, Yoo J, Quinn TP, Welch MJ, Lewis JS. Imaging of melanoma using ⁶⁴Cu- and ⁸⁶Y-DOTA-ReCCMSH(Arg11), a cyclized peptide analogue of alpha-MSH. *J Med Chem.* 2005;48:2985–92.
68. Rogers BE, Bigott HM, McCarthy DW, Della Manna D, Kim J, Sharp TL, et al. MicroPET imaging of a gastrin-releasing peptide receptor-positive tumor in a mouse model of human prostate cancer using a ⁶⁴Cu-labeled bombesin analogue. *Bioconjug Chem.* 2003;14:756–63.
69. Cheng Z, Zhang L, Graves E, Xiong Z, Dandekar M, Chen X, et al. Small-animal PET of melanocortin 1 receptor expression using a ¹⁸F-labeled alpha-melanocyte-stimulating hormone analog. *J Nucl Med.* 2007;48:987–94.
70. Ren G, Liu Z, Miao Z, Liu H, Subbarayan M, Chin FT, et al. PET of malignant melanoma using ¹⁸F-labeled metalloprotein. *J Nucl Med.* 2009;50:1865–72.
71. Ren G, Liu S, Liu H, Miao Z, Cheng Z. Radiofluorinated rhenium cyclized alpha-MSH analogues for PET imaging of melanocortin receptor 1. *Bioconjug Chem.* 2010;21:2355–60.
72. Jiang H, Kasten BB, Liu H, Qi S, Liu Y, Tian M, et al. Novel, cysteine-modified chelation strategy for the incorporation of [MCO₃](+) (M = Re, ^{99m}Tc) in an alpha-MSH peptide. *Bioconjug Chem.* 2012;23:2300–12.
73. Kasten BB, Ma X, Liu H, Hayes TR, Barnes CL, Qi S, et al. Clickable, hydrophilic ligand for fac-[MCO₃](+) (M = Re/^{99m}Tc) applied in an S-functionalized alpha-MSH peptide. *Bioconjug Chem.* 2014;25:579–92.
74. Guo H, Yang J, Gallazzi F, Miao Y. Effects of the amino acid linkers on the melanoma-targeting and pharmacokinetic properties of ¹¹¹In-labeled lactam bridge-cyclized alpha-MSH peptides. *J Nucl Med.* 2011;52:608–16.
75. Guo H, Gallazzi F, Miao Y. Gallium-67-labeled lactam bridge-cyclized alpha-MSH peptides with enhanced melanoma uptake and reduced renal uptake. *Bioconjug Chem.* 2012;23:1341–8.
76. Guo H, Miao Y. Cu-64-labeled lactam bridge-cyclized alpha-MSH peptides for PET imaging of melanoma. *Mol Pharm.* 2012;9:2322–30.
77. Yang J, Xu J, Gonzalez R, Lindner T, Kratochwil C, Miao Y. (68)Ga-DOTA-GGNle-CycMSH targets the melanocortin-1 receptor for melanoma imaging. *Sci Transl Med.* 2018;10:eaa4445.
78. Zhang C, Zhang Z, Lin KS, Lau J, Zeisler J, Colpo N, et al. Melanoma imaging using ¹⁸F-labeled alpha-melanocyte-stimulating hormone derivatives with positron emission tomography. *Mol Pharm.* 2018;15:2116–22.
79. Qiao Z, Xu J, Gonzalez R, Miao Y. Novel ⁶⁴Cu-labeled NOTA-conjugated lactam-cyclized alpha-melanocyte-stimulating hormone peptides with enhanced tumor to kidney uptake ratios. *Mol Pharm.* 2022;19:2535–41.
80. Miao Y, Quinn TP. Peptide-targeted radionuclide therapy for melanoma. *Crit Rev Oncol Hematol.* 2008;67:213–28.
81. Norain A, Dadachova E. Targeted radionuclide therapy of melanoma. *Semin Nucl Med.* 2016;46:250–9.
82. Miao Y, Quinn TP. Advances in receptor-targeted radiolabeled peptides for melanoma imaging and therapy. *J Nucl Med.* 2021;62:313–8.
83. Simon JD. Spectroscopic and dynamic studies of the epidermal chromophores trans-urocanic acid and eumelanin. *Acc Chem Res.* 2000;33:307–13.
84. Noonan FP, Zaidi MR, Wolnicka-Glubisz A, Anver MR, Bahn J, Wielgus A, et al. Melanoma induction by ultraviolet A but not ultraviolet B radiation requires melanin pigment. *Nat Commun.* 2012;3:884.
85. Larsson BS. Interaction between chemicals and melanin. *Pigment Cell Res.* 1993;6:127–33.
86. Jimbow K, Quevedo WC Jr, Fitzpatrick TB, Szabo G. Some aspects of melanin biology: 1950–1975. *J Invest Dermatol.* 1976;67:72–89.
87. Ings RMJ. The melanin binding of drugs and its implications. *Drug Metab Rev.* 1984;15:1183–212.
88. Koch SE, Lange JR. Amelanotic melanoma: the great masquerader. *J Am Acad Dermatol.* 2000;42:731–4.
89. Wee E, Wolfe R, McLean C, Kelly JW, Pan Y. Clinically amelanotic or hypomelanotic melanoma: anatomic distribution, risk factors, and survival. *J Am Acad Dermatol.* 2018;79:645–51.
90. Slominski RM, Zmijewski MA, Slominski AT. The role of melanin pigment in melanoma. *Exp Dermatol.* 2015;24:258–9.
91. Brozyna AA, Jozwicki W, Roszkowski K, Filipiak J, Slominski AT. Melanin content in melanoma metastases affects the outcome of radiotherapy. *Oncotarget.* 2016;7:17844–53.
92. Rouanet J, Quintana M, Auzeloux P, Cachin F, Degoul F. Benzamide derivative radiotracers targeting melanin for melanoma imaging and therapy: preclinical/clinical development and combination with other treatments. *Pharmacol Ther.* 2021;224:107829.
93. Link E, Lukiewicz S. A new radioactive drug selectively accumulating in melanoma-cells. *Eur J Nucl Med.* 1982;7:469–73.
94. Michelot JM, Moreau MC, Labarre PG, Madelmont JC, Veyre AJ, Papon JM, et al. Synthesis and evaluation of new iodine-125 radiopharmaceuticals as potential tracers for malignant melanoma. *Nucl Med.* 1991;32:1573–80.
95. Michelot JM, Moreau MF, Veyre AJ, Bonafous JF, Bacin FJ, Madelmont JC, et al. Phase II scintigraphic clinical trial of malignant melanoma and metastases with iodine-123-N-(2-diethylaminoethyl 4-iodobenzamide). *J Nucl Med.* 1993;34:1260–6.
96. Moins N, D'Incan M, Bonafous J, Bacin F, Labarre P, Moreau MF, et al. 123I-N-(2-diethylaminoethyl)-2-iodobenzamide: a potential imaging agent for cutaneous melanoma staging. *Eur J Nucl Med Mol Imaging.* 2002;29:1478–84.
97. Cachin F, Miot-Noirault E, Gillet B, Isnardi V, Labelle B, Payoux P, et al. ¹²³I-BZA2 as a melanin-targeted radiotracer for the identification of melanoma metastases: results and perspectives of a multicenter phase III clinical trial. *J Nucl Med.* 2014;55:15–22.
98. Ren G, Miao Z, Liu H, Jiang L, Limpia-Amara N, Mahmood A, et al. Melanin-targeted preclinical PET imaging of melanoma metastasis. *J Nucl Med.* 2009;50:1692–9.

99. Greguric I, Taylor SR, Denoyer D, Ballantyne P, Berghofer P, Roselt P, et al. Discovery of [^{18}F]N-(2-(Diethylamino)ethyl)-6-fluoronicotinamide: a melanoma positron emission tomography imaging radiotracer with high tumor to body contrast ratio and rapid renal clearance. *J Med Chem.* 2009;52:5299–302.
100. Denoyer D, Greguric I, Roselt P, Neels OC, Aide N, Taylor SR, et al. High-contrast PET of melanoma using ^{18}F -MEL050, a selective probe for melanin with predominantly renal clearance. *J Nucl Med.* 2010;51:441–7.
101. Liu H, Liu S, Miao Z, Deng Z, Shen B, Hong X, et al. Development of ^{18}F -labeled picolinamide probes for PET imaging of malignant melanoma. *J Med Chem.* 2013;56:895–901.
102. Qin C, Cheng K, Chen K, Hu X, Liu Y, Lan X, et al. Tyrosinase as a multifunctional reporter gene for photoacoustic/MRI/PET triple modality molecular imaging. *Sci Rep.* 2013;3:1490.
103. Bu L, Li R, Liu H, Feng W, Xiong X, Zhao H, et al. Intrastriatal transplantation of retinal pigment epithelial cells for the treatment of Parkinson disease: in vivo longitudinal molecular imaging with ^{18}F -P3BZA PET/CT. *Radiology.* 2014;272:174–83.
104. Liu H, Liu S, Miao Z, Jiang H, Deng Z, Hong X, et al. A novel aliphatic ^{18}F -labeled probe for PET imaging of melanoma. *Mol Pharmacol.* 2013;10:3384–91.
105. Ma X, Wang S, Wang S, Liu D, Zhao X, Chen H, et al. Biodistribution, radiation dosimetry, and clinical application of a melanin-targeted PET probe, ^{18}F -P3BZA, in patients. *J Nucl Med.* 2019;60:16–22.
106. Hong Z, Yu B, Xiao J, Feng H, Ma X, Cheng Z, et al. A convenient and efficient solid phase extraction-based pathway for purification of melanin-targeted probe ^{18}F -P3BZA. *Microchem J.* 2021;164:106008.
107. Pyo A, Kim DY, Kim H, Lim D, Kwon SY, Kang SR, et al. Ultrasensitive detection of malignant melanoma using PET molecular imaging probes. *Proc Natl Acad Sci USA.* 2020;117:12991–9.
108. Zhang X, Li M, Gai Y, Chen J, Tao J, Yang L, et al. ^{18}F -PFPPN PET: a new and attractive imaging modality for patients with malignant melanoma. *J Nucl Med.* 2022;jnumed.121.263179.
109. Zhang X, Li M, Lan X. Melanin-targeted PET imaging with ^{18}F -PFPPN for identifying gastric metastatic melanoma. *Clin Nucl Med.* 2022;47:666–7.
110. Fan Q, Cheng K, Hu X, Ma X, Zhang R, Yang M, et al. Transferring biomarker into molecular probe: melanin nanoparticle as a naturally active platform for multimodality imaging. *J Am Chem Soc.* 2014;136:15185–94.
111. Yang M, Fan Q, Zhang R, Cheng K, Yan J, Pan D, et al. Dragon fruit-like biocage as an iron trapping nanoparticle for high efficiency targeted cancer multimodality imaging. *Biomaterials.* 2015;69:30–7.
112. Zhang R, Fan Q, Yang M, Cheng K, Lu X, Zhang L, et al. Engineering melanin nanoparticles as an efficient drug-delivery system for imaging-guided chemotherapy. *Adv Mater.* 2015;27:5063–9.
113. Hong SH, Sun Y, Tang C, Cheng K, Zhang R, Fan Q, et al. Chelator-free and biocompatible melanin nanoparticle platform with facile-loading gadolinium and copper-64 for bioimaging. *Bioconjug Chem.* 2017;28:1925–30.
114. Xia L, Guo X, Liu T, Xu X, Jiang J, Wang F, et al. Multimodality imaging of naturally active melanin nanoparticles targeting somatostatin receptor subtype 2 in human small-cell lung cancer. *Nanoscale.* 2019;11:14400–9.
115. Shi H, Suo Y, Zhang Z, Liu R, Liu H, Cheng Z. Copper(II)-disulfiram loaded melanin-dots for cancer theranostics. *Nanomedicine.* 2021;32:102340.
116. Sun T, Jiang D, Rosenkrans ZT, Ehlerding EB, Ni D, Qi C, et al. A melanin-based natural antioxidant defense nanosystem for theranostic application in acute kidney injury. *Adv Funct Mater.* 2019;29:1904833.
117. Xia L, Meng X, Wen L, Zhou N, Liu T, Xu X, et al. A highly specific multiple enhancement theranostic nanoprobe for PET/MRI/PAI image-guided radioisotope combined photothermal therapy in prostate cancer. *Small.* 2021;17:e2100378.
118. Zhao X, Sun J, Dong J, Guo C, Cai W, Han J, et al. An auto-photoacoustic melanin-based drug delivery nano-platform for self-monitoring of acute kidney injury therapy via a triple-collaborative strategy. *Acta Biomater.* 2022;147:327–41.
119. Ball V. Polydopamine films and particles with catalytic activity. *Catal Today.* 2018;301:196–203.
120. Ball V. Polydopamine nanomaterials: recent advances in synthesis methods and applications. *Front Bioeng Biotechnol.* 2018;6:109.
121. Ryu JH, Messersmith PB, Lee H. Polydopamine surface chemistry: a decade of discovery. *ACS Appl Mater Interfaces.* 2018;10:7523–40.
122. Ambekar RS, Kandasubramanian B. A polydopamine-based platform for anti-cancer drug delivery. *Biomater Sci.* 2019;7:1776–93.
123. Cheng W, Zeng X, Chen H, Li Z, Zeng W, Mei L, et al. Versatile polydopamine platforms: synthesis and promising applications for surface modification and advanced nanomedicine. *ACS Nano.* 2019;13:8537–65.
124. Huang Q, Chen J, Liu M, Huang H, Zhang X, Wei Y. Polydopamine-based functional materials and their applications in energy, environmental, and catalytic fields: state-of-the-art review. *Chem Eng J.* 2020;387:124019.
125. Lee HA, Park E, Lee H. Polydopamine and its derivative surface chemistry in material science: a focused review for studies at KAIST. *Adv Mater.* 2020;32:e1907505.
126. Palangka C, Hanaoka H, Yamaguchi A, Murakami T, Tsushima Y. Al ^{18}F -labeled alpha-melanocyte-stimulating hormone (alpha-MSH) peptide derivative for the early detection of melanoma. *Ann Nucl Med.* 2019;33:733–9.
127. Xu J, Yang J, Gonzalez R, Fisher DR, Miao Y. Melanoma-targeting property of Y-90-labeled lactam-cyclized alpha-melanocyte-stimulating hormone peptide. *Cancer Biother Radiopharm.* 2019;34:597–603.
128. Yang J, Xu J, Cheuy L, Gonzalez R, Fisher DR, Miao Y. Evaluation of a novel Pb-203-labeled lactam-cyclized alpha-melanocyte-stimulating hormone peptide for melanoma targeting. *Mol Pharm.* 2019;16:1694–702.
129. Qiao Z, Xu J, Gonzalez R, Miao Y. Novel [$^{99\text{m}}\text{Tc}$]-tricarboxyl-NOTA-conjugated lactam-cyclized alpha-MSH peptide with enhanced melanoma uptake and reduced renal uptake. *Mol Pharm.* 2020;17:3581–8.
130. Xu J, Qiao Z, Gonzalez R, Miao Y. Facile preparation of a novel Ga-67-labeled NODAGA-conjugated lactam-cyclized alpha-MSH peptide at room temperature for melanoma targeting. *Bioorg Med Chem Lett.* 2020;30:127627.
131. Garg S, Kothari K, Thopate SR, Doke AK, Garg PK. Design, synthesis, and preliminary in vitro and in vivo evaluation of N-(2-diethylaminoethyl)-4-[^{18}F]fluorobenzamide ([^{18}F]-DAFBA): a novel potential PET probe to image melanoma tumors. *Bioconjug Chem.* 2009;20:583–90.

Springer Nature or its licensor holds exclusive rights to this article under a publishing agreement with the author(s) or other rightsholder(s); author self-archiving of the accepted manuscript version of this article is solely governed by the terms of such publishing agreement and applicable law.